Journal of Computational and Applied Mathematics 350 (2019) 247–261

Contents lists available at ScienceDirect

Journal of Computational and Applied Mathematics

journal homepage: www.elsevier.com/locate/cam

High-order local discontinuous Galerkin method for simulating wormhole propagation☆

Hui Guo [a], Lulu Tian [a,*], Ziyao Xu [b], Yang Yang [b], Ning Qi [c]

[a] College of Science, China University of Petroleum, Qingdao 266580, China
[b] Michigan Technological University, Houghton, MI 49931, USA
[c] School of Petroleum Engineering, China University of Petroleum, Qingdao 266580, China

ARTICLE INFO

Article history:
Received 18 January 2018
Received in revised form 11 July 2018

MSC:
65M15
65M60

Keywords:
Local discontinuous Galerkin method
Error estimate
Compressible wormhole propagation

ABSTRACT

In this paper, we apply local discontinuous Galerkin methods to the compressible wormhole propagation. Optimal error estimates for the pressure, velocity, porosity and concentration in different norms are established on non-uniform grids. Numerical experiments are presented to verify the theoretical analysis and show the good performance of the LDG scheme for compressible wormhole propagation.

1. Introduction

To increase the production rate, acid treatment of carbonate reservoirs has been widely applied in oil and gas well stimulation techniques by increasing permeability of the damaged zone near the well. The material near the well can be dissolved by the injected acid and flow channels that establish a good connectivity between the reservoir and the well can be constructed. It is well known that the relative increase in permeability for a given amount of acid is a strong function of the injection conditions and only at suitable flow rates, wormholes (long conductive channels) are formed. These channels penetrate deep into the formation and facilitate the flow of oil. Thus, for successful stimulation of a well it is required to produce wormholes with optimum density and penetrating deep into the formation.

The mathematical model of the wormhole propagation has been investigated intensively [1–6]. To the best knowledge, there are not too many works discussing numerical simulations. Theoretical and numerical analyses of chemical-dissolution front instability were investigated in [7]. Later, parallel simulation for wormhole propagation was discussed in [8]. Subsequently, in [9], the authors applied the mixed finite element method to the problem. The stability analysis and a priori error estimates for velocity, pressure, concentration and porosity were established in different norms. Moreover, in [10] the authors considered block-centered finite difference method. However, the scheme is only second-order accurate. To the best

☆ The first author was supported by National Natural Science Foundation of China Grants 11571367 and the Fundamental Research Funds for the Central Universities 18CX05003A. The second author was supported by the Fundamental Research Funds for the Central Universities YJ201601010 and 18CX02021A. The fourth author was supported by NSF grant DMS-1818467. The last author was supported by the National Key Technologies Research and Development Program of China during the 13th Five-Year Plan Period (Project No. 2017ZX005030005) and Shandong Provincial Natural Science Foundation ZR2017MEE073.

* Corresponding author.
E-mail addresses: guohui@upc.edu.cn (H. Guo), Tianll@upc.edu.cn (L. Tian), ziyaox@mtu.edu (Z. Xu), yyang7@mtu.edu (Y. Yang), qining@upc.edu.cn (N. Qi).

https://doi.org/10.1016/j.cam.2018.10.021
0377-0427/

knowledge of the authors, no previous work focused on discontinuous Galerkin (DG) methods for wormhole propagation. In this paper, we would like to apply the high-order local discontinuous Galerkin (LDG) methods for compressible wormhole propagation.

The DG method gained even greater popularity recently for good stability, high order accuracy, and flexibility on h-p adaptivity and on complex geometry. The DG method was first introduced in 1973 by Reed and Hill [11] in the framework of neutron linear transport. Subsequently, Cockburn et al. developed Runge–Kutta discontinuous Galerkin (RKDG) methods for hyperbolic conservation laws in a series of papers [12–15]. In [16], Cockburn and Shu first introduced the local discontinuous Galerkin (LDG) method to solve the convection–diffusion equation. Their idea was motivated by Bassi and Rebay [17], where the compressible Navier–Stokes equations were successfully solved. The idea of the LDG method is to rewrite the equation with higher order derivatives into a first order system, then apply the DG method to the system. With suitable numerical fluxes, the stability and optimal error estimates can be proved for some model equations [18–21]. As an extension of DG schemes for hyperbolic conservation laws, the LDG methods share the advantages of the DG methods. Besides, a key advantage of this scheme is the local solvability, i.e. the auxiliary variables approximating the gradient of the solution can be locally eliminated.

It is not easy to apply the LDG methods to wormhole propagation directly due to the inter-element discontinuities of two independent solution variables. More precisely, in this problem, the approximations of $\mathbf{u}$ in the convection term in (2.3) is discontinuous across the cell interfaces and it is difficult to obtain the error estimates if we analyze the convection and diffusion terms separately. To explain this point, let us consider the following hyperbolic equation

$$u_t + (a(x)u)_x = 0,$$

where $a(x)$ is discontinuous at $x = x_0$. In [22,23], the authors studied such a problem and defined

$$Q = \frac{a(x_0 + b) - a(x_0)}{b}.$$

If Q is bounded from below for all b, then the solution exists, but may not be unique. If Q is bounded from above for all b, we can guarantee the uniqueness, but the solution may not exist. Recently, Wang et al. [24–26] obtained optimal error estimates of the LDG methods with IMEX time integration for linear and nonlinear convection–diffusion problems. Subsequently, the idea has been applied to miscible displacements in porous media [27–29], chemotaxis model [30] to obtain optimal rates of convergence. The key idea is to explore an important relationship between the gradient and interface jump of the numerical solution polynomial with the numerical approximation of auxiliary variable for the gradient in the LDG methods, which is stated in Lemma 4.4. Moreover, the systems are coupled together. Therefore, we will derive four energy inequalities to obtain optimal error estimates in $L^\infty(0, T; L^2)$ for concentration c, in $L^2(0, T; L^2)$ for $\mathbf{s} = -\nabla c$, in $L^\infty(0, T; L^2)$ for porosity ϕ and in $L^\infty(0, T; L^2)$ for pressure p.

The paper is organized as follows. In Section 2, we demonstrate the governing equations of the compressible wormhole propagation. In Section 3, we present some preliminaries, including the basic notations and norms to be used throughout the paper and the LDG spatial discretization. Section 4 is the main body of the paper where we present the projections and some essential properties of the finite element spaces, error equations and the details of the optimal error estimates for compressible wormhole propagation. Numerical results are given to demonstrate the accuracy and capability of the method in Section 5. We will end in Section 6 with some concluding remarks.

2. Compressible wormhole propagation

In this section, we demonstrate the governing equations of the compressible wormhole propagation. Let $\Omega = [0, 1] \times [0, 1]$ be a rectangular domain in R^2. The classical equations governing the compressible wormhole propagation in two space dimensions are as follows [9,10]:

$$\gamma \frac{\partial p}{\partial t} + \frac{\partial \phi}{\partial t} + \nabla \cdot \mathbf{u} = f, \quad (x, y) \in \Omega,\ 0 < t \le T, \tag{2.1}$$

$$\mathbf{u} = \frac{-\kappa(\phi)}{\mu} \nabla p, \quad (x, y) \in \Omega,\ 0 < t \le T, \tag{2.2}$$

$$\frac{\partial (\phi c_f)}{\partial t} + \nabla \cdot (\mathbf{u} c_f) = \nabla \cdot (\phi \mathbf{D} \nabla c_f) + k_c a_v (c_s - c_f) + f_p c_f + f_I c_I, \tag{2.3}$$

$$\frac{\partial \phi}{\partial t} = \frac{\alpha k_c a_v (c_f - c_s)}{\rho_s}, \quad (x, y) \in \Omega,\ 0 < t \le T, \tag{2.4}$$

where p and $\mathbf{u}$ are the pressure in the fluid mixture, the Darcy velocity of the mixture (volume flowing across a unit cross-section per unit time), respectively. μ is the viscosity and γ is a pseudo-compressibility parameter that results in slight change of the density of the fluid phase in the dissolution process. $f = f_I + f_p$ is the external volumetric flow rate with f_P and f_I being the production and injection rates, respectively. c_f is the cup-mixing concentration of the acid in the fluid phase. c_I is the injected concentration. Following [10], we consider only molecular diffusion, so that $\mathbf{D} = d_m I$ with I being the identity matrix. In this paper the tensor matrix $\mathbf{D}$ is assumed to be positive definite and may depend on x, y, but not $\mathbf{u}$. Moreover, the pressure is uniquely determined up to a constant, thus we assume $\int_\Omega p dxdy = 0$ at $t = 0$. k_c is the local mass-transfer

coefficient, a_v is the interfacial area available for reaction per unit volume of the medium. The variable c_s is the concentration of the acid at the fluid–solid interface given as

$$c_s = \frac{c_f}{1 + k_s/k_c}, \tag{2.5}$$

where k_s is the surface reaction rate constant. ϕ and κ in the first term on the right hand side of (2.2) are the porosity and permeability of the rock, respectively and the relationship between the permeability and the porosity is established by the Carman–Kozeny correlation [31]

$$\frac{\kappa}{\kappa_0} = \frac{\phi}{\phi_0}\left(\frac{\phi(1-\phi_0)}{\phi_0(1-\phi)}\right)^2, \tag{2.6}$$

where ϕ_0 and κ_0 are the initial porosity and permeability of the rock, respectively. Therefore, we can consider κ as a function of ϕ, and it is easy to derive

$$\frac{1}{\kappa(\phi)} = \kappa^{-1}(\phi) = \frac{\phi_0}{\phi\kappa_0}\left(\frac{\phi_0(1-\phi)}{\phi(1-\phi_0)}\right)^2.$$

In (2.4), α is the dissolving power of the acid and ρ_s is the density of the solid phase. Using porosity and permeability, a_v is shown as

$$\frac{a_v}{a_0} = \frac{\phi}{\phi_0}\sqrt{\frac{\kappa_0\phi}{\kappa\phi_0}} = \frac{1-\phi}{1-\phi_0}, \tag{2.7}$$

where a_0 is the initial interfacial area. In this problem, the initial concentration are pressure are given as

$$c_f(x, y, 0) = c_0(x, y), \quad p(x, y, 0) = p_0(x, y), \quad \phi(x, y, 0) = \phi_0(x, y), \quad (x, y) \in \Omega.$$

For simplicity, we consider periodic boundary condition in this paper. The analysis for homogeneous Neumann boundary can be obtained following the same lines with some minor changes, and we thus omit it.

Finally, we make the following hypotheses (H) for the problem.

1. $0 < \phi_* \le \phi(x, y) \le \phi^* < 1$.
2. $\mathbf{D}$ is uniformly Lipschitz continuous, and for any $\mathbf{v}, \mathbf{w} \in R^2$ there exist two positive constants D_*, D^* such that $\mathbf{v}^T\mathbf{D}\mathbf{v} \ge D_*\mathbf{v}^T\mathbf{v} = D_*\|\mathbf{v}\|^2$ and $\mathbf{v}^T\mathbf{D}\mathbf{w} \le D^*\|\mathbf{v}\|\|\mathbf{w}\|$, where $\|\mathbf{v}\|$ is the standard Euclidian norm in R^2.
3. γ, α, ρ_s, μ, k_c, and k_s are all given positive constants, and $0 < \phi_{0*} \le \phi_0 \le \phi_0^* < 1$, $0 < a_{0*} \le a_0 \le a_0^*$.
4. c_f, ϕ, c_{f_t}, ϕ_t, $\mathbf{u}$ and $\mathbf{s} = -\nabla c_f$ are uniformly bounded in $R^2 \times [0, T]$.

It is easy to obtain the following lemma

Lemma 2.1. *Suppose hypotheses 1 and 3 are satisfied, then $a_v(\phi)$ and $\kappa^{-1}(\phi)$ are bounded and Lipschitz continuous, i.e. there exists C such that*

$$a_v(\phi) \le C, \quad \kappa^{-1}(\phi) \le C, \quad |a_v(\phi_1) - a_v(\phi_2)| \le C|\phi_1 - \phi_2| \quad |\kappa^{-1}(\phi_1) - \kappa^{-1}(\phi_2)| \le C|\phi_1 - \phi_2|.$$

3. Preliminaries

In this section, we will demonstrate some preliminary results that will be used throughout the paper.

3.1. Basic notations

In this section, we present the notations. Let $0 = x_{\frac{1}{2}} < \cdots < x_{N_x+\frac{1}{2}} = 1$ and $0 = y_{\frac{1}{2}} < \cdots < y_{N_y+\frac{1}{2}} = 1$ be the grid points in the x and y directions, respectively. Define $I_i = (x_{i-\frac{1}{2}}, x_{i+\frac{1}{2}})$ and $J_j = (y_{j-\frac{1}{2}}, y_{j+\frac{1}{2}})$. Let $K = I_i \times J_j$, $i = 1, \ldots, N_x$, $j = 1, \ldots, N_y$, be a partition of Ω and denote $\Omega_h = \{K\}$. The mesh sizes in the x and y directions are given as $\Delta x_i = x_{i+\frac{1}{2}} - x_{i-\frac{1}{2}}$ and $\Delta y_j = y_{j+\frac{1}{2}} - y_{j-\frac{1}{2}}$, respectively and $h = \max\{\max_i \Delta x_i, \max_j \Delta y_j\}$. Moreover, we assume the partition is quasi-uniform, i.e. there exists a positive constant λ such that $h \le \lambda h_{min}$, where $h_{min} = \min\{\min_i \Delta x_i, \min_j \Delta y_j\}$. The finite element space is chosen as

$$W_h^k = \{z : z|_K \in Q^k(K), \forall K \in \Omega_h\},$$

where $Q^k(K)$ denotes the space of tensor product polynomials of degrees at most k in K. Note that functions in W_h^k are discontinuous across element interfaces. This is one of the main differences between the DG method and traditional finite element method. We choose $\boldsymbol{\beta} = (1, 1)^T$ to be a fixed vector that is not parallel to any normals of the element interfaces. We denote Γ_h to be the set of all element interfaces and $\Gamma_0 = \Gamma_h \backslash \partial\Omega$. Let $\mathcal{E} \in \Gamma_0$ be an interior edge shared by elements K_ℓ and K_r, where $\boldsymbol{\beta} \cdot \mathbf{n}_\ell > 0$, and $\boldsymbol{\beta} \cdot \mathbf{n}_r < 0$, respectively, with $\mathbf{n}_\ell$ and $\mathbf{n}_r$ being the outward normals of K_ℓ and K_r, respectively.

For any $z \in W_h^k$, we define $z^- = z|_{\partial K_\ell}$ and $z^+ = z|_{\partial K_r}$, respectively. The jump is given as $[z] = z^+ - z^-$. Moreover, for $\mathbf{s} \in \mathbf{W}_h^k = W_h^k \times W_h^k$, we define $\mathbf{s}^+$ and $\mathbf{s}^-$ and $[\mathbf{s}]$ analogously. We also define $\partial\Omega_- = \{\mathcal{E} \in \partial\Omega | \boldsymbol{\beta} \cdot \mathbf{n} < 0\}$, where $\mathbf{n}$ is the outer normal of $\mathcal{E}$, and $\partial\Omega_+ = \partial\Omega \backslash \partial\Omega_-$. For any $\mathcal{E} \in \partial\Omega_-$, there exists $K \in \Omega_h$ such that $\mathcal{E} \in \partial K$, we define $z^+|_{\mathcal{E}} = z|_{\partial K}$, and define z^- on $\partial\Omega_+$ analogously. For simplicity, given $\mathcal{E} = \{x_{\frac{1}{2}}\} \times J_j \in \partial\Omega_-$ and $\tilde{\mathcal{E}} = \{x_{N_x+\frac{1}{2}}\} \times J_j \in \partial\Omega_+$, by periodic boundary condition, we define

$$z^-|_{\mathcal{E}} = z^-|_{\tilde{\mathcal{E}}}, \quad \text{and} \quad z^+|_{\tilde{\mathcal{E}}} = z^+|_{\mathcal{E}}.$$

Similarly, given $\mathcal{E} = I_i \times \{y_{\frac{1}{2}}\} \in \partial\Omega_-$ and $\tilde{\mathcal{E}} = I_i \times \{y_{N_y+\frac{1}{2}}\} \in \partial\Omega_+$, we define

$$z^-|_{\mathcal{E}} = z^-|_{\tilde{\mathcal{E}}}, \quad \text{and} \quad z^+|_{\tilde{\mathcal{E}}} = z^+|_{\mathcal{E}}.$$

Throughout this paper, the symbol C is used as a generic constant which may appear differently at different occurrences. Moreover, the symbol ϵ is a sufficiently small positive constant.

3.2. Norms

In this subsection, we define several norms that will be used throughout the paper.

Denote $\|u\|_{0,K}$ to be the standard L^2 norm of u in cell K. For any natural number ℓ, we consider the norm of the Sobolev space $H^\ell(K)$, defined by

$$\|u\|_{\ell,K} = \left\{ \sum_{0 \le \alpha+\beta \le \ell} \left\| \frac{\partial^{\alpha+\beta} u}{\partial x^\alpha \partial y^\beta} \right\|_{0,K}^2 \right\}^{\frac{1}{2}}.$$

Moreover, we define the norms on the whole computational domain as

$$\|u\|_\ell = \left(\sum_{K \in \Omega_h} \|u\|_{\ell,K}^2 \right)^{\frac{1}{2}}.$$

For convenience, if we consider the standard L^2 norm, then the corresponding subscript will be omitted.

Let Γ_K be the edges of K, and we define

$$\|u\|_{\Gamma_K}^2 = \int_{\partial K} u^2 ds.$$

We also define

$$\|u\|_{\Gamma_h}^2 = \sum_{K \in \Omega_h} \|u\|_{\Gamma_K}^2.$$

Moreover, we define the standard L^∞ norm of u in K as $\|u\|_{\infty,K}$, and define the L^∞ norm on the whole computational domain as

$$\|u\|_\infty = \max_{K \in \Omega_h} \|u\|_{\infty,K}.$$

Finally, we define similar norms for vector $\mathbf{u} = (u_1, u_2)^T$ as

$$\|\mathbf{u}\|_{\ell,K}^2 = \|u_1\|_{\ell,K}^2 + \|u_2\|_{\ell,K}^2, \quad \|\mathbf{u}\|_{\Gamma_K}^2 = \|u_1\|_{\Gamma_K}^2 + \|u_2\|_{\Gamma_K}^2, \quad \|\mathbf{u}\|_{\infty,K} = \max\{\|u_1\|_{\infty,K}, \|u_2\|_{\infty,K}\}.$$

Similarly, the norms on the whole computational domain are given as

$$\|\mathbf{u}\|_\ell^2 = \sum_{K \in \Omega_h} \|\mathbf{u}\|_{\ell,K}^2, \quad \|\mathbf{u}\|_{\Gamma_h}^2 = \sum_{K \in \Omega_h} \|\mathbf{u}\|_{\Gamma_K}^2, \quad \|\mathbf{u}\|_\infty = \max_{K \in \Omega_h} \|\mathbf{u}\|_{\infty,K}.$$

3.3. LDG scheme

Applying (2.5)–(2.7), we can transform the nonlinear system (2.1)–(2.4) into

$$\gamma \frac{\partial p}{\partial t} + \frac{\partial \phi}{\partial t} + \nabla \cdot \mathbf{u} = f, \tag{3.1}$$

$$\mathbf{u} = \frac{-\kappa(\phi)}{\mu} \nabla p, \tag{3.2}$$

$$\frac{\partial(\phi c_f)}{\partial t} + \nabla \cdot (\mathbf{u} c_f) - \nabla \cdot (\phi \mathbf{D} \nabla c_f) + A a_v(\phi) c_f = f_p c_f + f_I c_I, \tag{3.3}$$

$$\frac{\partial \phi}{\partial t} = Ba_v(\phi)c_f, \tag{3.4}$$

where $A = \frac{k_c k_s}{k_c+k_s}$, $B = \frac{\alpha k_c k_s}{\rho_s(k_c+k_s)}$ and $a_v(\phi) = \frac{a_0(1-\phi)}{1-\phi_0}$. Then we introduce some auxiliary variables to represent the derivatives of the solution which further yields a first order system:

$$\gamma \frac{\partial p}{\partial t} + \frac{\partial \phi}{\partial t} + \nabla \cdot \mathbf{u} = f, \tag{3.5}$$

$$\frac{\mu}{\kappa(\phi)}\mathbf{u} + \nabla p = 0, \tag{3.6}$$

$$\frac{\partial(\phi c_f)}{\partial t} + \nabla \cdot (\mathbf{u}c_f) + \nabla \cdot \mathbf{z} + Aa_v(\phi)c_f = f_p c_f + f_I c_I, \tag{3.7}$$

$$\mathbf{s} = -\nabla c_f, \tag{3.8}$$

$$\mathbf{z} = \phi \mathbf{D}\mathbf{s}, \tag{3.9}$$

$$\frac{\partial \phi}{\partial t} = Ba_v(\phi)c_f. \tag{3.10}$$

We multiply (3.5)–(3.10) with test functions and formally integrate by parts in K to obtain

$$\begin{aligned}
\left(\gamma \frac{\partial p}{\partial t}, \zeta\right)_K + \left(\frac{\partial \phi}{\partial t}, \zeta\right)_K &= (\mathbf{u}, \nabla\zeta)_K - \langle \mathbf{u}\cdot\boldsymbol{\nu}_K, \zeta\rangle_{\partial K} + (f, \zeta)_K,\\
\left(\frac{\mu}{\kappa(\phi)}\mathbf{u}, \boldsymbol{\theta}\right)_K &= (p, \nabla\cdot\boldsymbol{\theta})_K - \langle p, \boldsymbol{\theta}\cdot\boldsymbol{\nu}_K\rangle_{\partial K},\\
((\phi c_f)_t, v)_K &= (\mathbf{u}c_f + \mathbf{z}, \nabla v)_K - \langle(\mathbf{u}c_f + \mathbf{z})\cdot\boldsymbol{\nu}_K, v\rangle_{\partial K}\\
&\quad - (Aa_v(\phi)c_f, v)_K + (f_p c_f + f_I c_I, v)_K,\\
(\mathbf{s}, \mathbf{w})_K &= (c_f, \nabla\cdot\mathbf{w})_K - \langle c_f, \mathbf{w}\cdot\boldsymbol{\nu}_K\rangle_{\partial K},\\
(\mathbf{z}, \boldsymbol{\psi})_K &= (\phi\mathbf{D}\mathbf{s}, \boldsymbol{\psi})_K,\\
(\phi_t, \beta)_K &= (Ba_v(\phi)c_f, \beta)_K,
\end{aligned}$$

where $\zeta, v, \beta \in W_h^k$, $\boldsymbol{\theta}, \mathbf{w}, \boldsymbol{\psi} \in \mathbf{W}_h^k$, $(u,v)_K = \int_K uv dxdy$, $(\mathbf{u},\mathbf{v})_K = \int_K \mathbf{u}\cdot\mathbf{v}dxdy$, $\langle u, v\rangle_{\partial K} = \int_{\partial K} uv ds$ and $\boldsymbol{\nu}_K$ is the outer unit normal of K. Replacing the exact solutions $c_f,\ p,\ \phi,\ \mathbf{s},\ \mathbf{z},\ \mathbf{u}$ in the above equations by their numerical approximations $c_h,\ p_h,\ \phi_h \in W_h^k$ and $\mathbf{s}_h,\ \mathbf{z}_h,\ \mathbf{u}_h \in \mathbf{W}_h^k$, respectively and using numerical fluxes along the cell interfaces, we can obtain the LDG scheme: for any $t \in [0, T]$,

$$\left(\gamma \frac{\partial p_h}{\partial t}, \zeta\right)_K + \left(\frac{\partial \phi_h}{\partial t}, \zeta\right)_K = \mathcal{L}_K^d(\mathbf{u}_h, \zeta) + (f, \zeta)_K \tag{3.11}$$

$$\left(\frac{\mu}{\kappa(\phi_h)}\mathbf{u}_h, \boldsymbol{\theta}\right)_K = \mathcal{D}_K(p_h, \boldsymbol{\theta}) \tag{3.12}$$

$$\begin{aligned}
((\phi c_f)_t, v)_K &= \mathcal{L}_K^c(\mathbf{u}_h, c_h, v) + \mathcal{L}_K^d(\mathbf{z}_h, v)\\
&\quad + (f_p c_h + f_I c_I, v)_K - (Aa_v(\phi_h)c_h, v)_K
\end{aligned} \tag{3.13}$$

$$(\mathbf{s}_h, \mathbf{w})_K = \mathcal{D}_K(c_h, \mathbf{w}) \tag{3.14}$$

$$(\mathbf{z}_h, \boldsymbol{\psi})_K = (\phi_h \mathbf{D}\mathbf{s}_h, \boldsymbol{\psi})_K \tag{3.15}$$

$$(\phi_{h_t}, \beta)_K = (Ba_v(\phi_h)c_h, \beta)_K \tag{3.16}$$

where

$$\begin{aligned}
\mathcal{L}_K^c(\mathbf{s}, c, v) &= (\mathbf{s}c, \nabla v)_K - \langle \widehat{\mathbf{s}c}\cdot\boldsymbol{\nu}_K, v\rangle_{\partial K},\\
\mathcal{L}_K^d(\mathbf{s}, v) &= (\mathbf{s}, \nabla v)_K - \langle \widehat{\mathbf{s}}\cdot\boldsymbol{\nu}_K, v\rangle_{\partial K},\\
\mathcal{D}_K(c, \mathbf{w}) &= (c, \nabla\cdot\mathbf{w})_K - \langle \widehat{c}, \mathbf{w}\cdot\boldsymbol{\nu}_K\rangle_{\partial K}.
\end{aligned}$$

The main error estimate requires the following initial discretization whose proof follows from Lemma 4.2 directly, and we thus omit it.

3.4. The main theorem

We will use several special projections in this paper. Firstly, we define P^+ into W_h^k which is, for each cell K

$$\begin{aligned}
&(P^+u - u, v)_K = 0, \quad \forall v \in Q^{k-1}(K),\\
&\int_{J_j} (P^+u - u)(x_{i-\frac{1}{2}}, y)v(y)dy = 0, \quad \forall v \in P^{k-1}(J_j),
\end{aligned}$$

$$\int_{I_i}(P^+u-u)(x,y_{j-\frac{1}{2}})v(x)dx=0,\quad \forall v\in P^{k-1}(I_i),$$
$$(P^+u-u)(x_{i-\frac{1}{2}},y_{j-\frac{1}{2}})=0,$$

where P^k denotes the polynomials of degree k. Moreover, we also define Π_x^- and Π_y^- into W_h^k which are, for each cell K,

$$(\Pi_x^-u-u,v_x)_K=0,\quad \forall v\in Q^k(K),$$
$$\int_{J_j}(\Pi_x^-u-u)(x_{i+\frac{1}{2}},y)v(y)dy=0,\quad \forall v\in P^k(J_j),$$
$$(\Pi_y^-u-u,v_y)_K=0,\quad \forall v\in Q^k(K),$$
$$\int_{I_i}(\Pi_y^-u-u)(x,y_{j+\frac{1}{2}})v(x)dx=0,\quad \forall v\in P^k(I_i),$$

as well as a vectored-valued projection $\boldsymbol{\Pi}^-=\Pi_x^-\otimes\Pi_y^-$. Finally, we also use the L^2-projection P_k into W_h^k which is, for each cell K

$$(P_ku-u,v)_K=0,\quad \forall v\in Q^k(K), \tag{3.17}$$

and its two dimensional version $\mathbf{P}_k=P_k\otimes P_k$. For the special projections given above, we will demonstrate the following lemma by the standard approximation theory [32].

Lemma 3.1. *We choose the initial solution as*

$$c_h(x,y,0)=P^+c_0,\quad \phi_h(x,y,0)=P_k\phi_0\quad p_h(x,y,0)=P^+p_0, \tag{3.18}$$

then we have

$$\|c_f(x,y,0)-c_h(x,y,0)\|\le Ch^{k+1},$$
$$\|p(x,y,0)-p_h(x,y,0)\|\le Ch^{k+1},$$
$$\|\phi(x,y,0)-\phi_h(x,y,0)\|\le Ch^{k+1}.$$

We use alternating fluxes for the diffusion term and take

$$\widehat{\mathbf{z}_h}=\mathbf{z}_h^-,\quad \widehat{c_h}=c_h^+,\quad \widehat{\mathbf{u}_h}=\mathbf{u}_h^-,\quad \widehat{p_h}=p_h^+.$$

For the convection term, we take

$$\widehat{\mathbf{u}_hc_h}=\frac{1}{2}(\mathbf{u}_h^+c_h^++\mathbf{u}_h^-c_h^--\alpha\boldsymbol{\nu}_e(c_h^+-c_h^-)),$$

where $\alpha\ge 0$ can be chosen as any fixed constant independent of h and $\boldsymbol{\nu}_e$ is the unit normal of $e\in\Gamma_0$ such that $\boldsymbol{\beta}\cdot\boldsymbol{\nu}_e>0$. Moreover, we define

$$(u,v)=\sum_{K\in\Omega_h}(u,v)_K,\qquad (\mathbf{u},\mathbf{v})=\sum_{K\in\Omega_h}(\mathbf{u},\mathbf{v})_K,$$

and

$$\mathcal{L}^c(\mathbf{s},c,v)=\sum_{K\in\Omega_h}\mathcal{L}_K^c(\mathbf{s},c,v),\qquad \mathcal{L}^d(\mathbf{s},v)=\sum_{K\in\Omega_h}\mathcal{L}_K^d(\mathbf{s},v),\qquad \mathcal{D}(c,\mathbf{w})=\sum_{K\in\Omega_h}\mathcal{D}_K(c,\mathbf{w}).$$

It is easy to check the following identity by integration by parts on each cell

Lemma 3.2. *For any functions v and $\mathbf{w}$,*

$$\mathcal{L}^d(\mathbf{w},v)+\mathcal{D}(v,\mathbf{w})=0. \tag{3.19}$$

Now we state the main theorem.

Theorem 3.1. *Let $c_f\in L^\infty(0,T;H^{k+3})$, $\boldsymbol{s}\in L^\infty(0,T;(H^{k+2})^2)$, $\boldsymbol{u}\in L^\infty(0,T;(H^{k+2})^2)$, $\phi\in L^\infty(0,T;H^{k+3})$ be the exact solutions of the problem (3.5)–(3.10), and let $\mathbf{u}_h$, p_h, c_h, $\mathbf{s}_h$, $\mathbf{z}_h$, ϕ_h be the numerical solutions of the semi-discrete LDG scheme (3.11)–(3.16) with initial discretization given as (3.18). If the finite element space is the piecewise tensor product polynomials of degree at most k and h is sufficiently small, then we have the error estimate*

$$\|c_f-c_h\|_{L^\infty(0,T;L^2)}+\|\mathbf{s}-\mathbf{s}_h\|_{L^2(0,T;L^2)}$$
$$+\|p-p_h\|_{L^\infty(0,T;L^2)}+\|\phi-\phi_h\|_{L^\infty(0,T;L^2)}\le Ch^{k+1}, \tag{3.20}$$

where the constant C is independent of h.

4. The proof of the main theorem

In this section, we proceed to the proof of Theorem 3.1. We first introduce several projections and present some auxiliary results. Subsequently, we make an a priori error estimate which provides the boundedness of the numerical approximations. Then we construct the error equations which further yield several main energy inequalities and complete the proof of (3.20). Finally, we verify the a priori error estimate at the end of this section.

4.1. Projections and interpolation properties

In this section, we will demonstrate the projections and several useful lemmas. Let us start with the classical inverse properties [32].

Lemma 4.1. *Assume $u \in W_h^k$, then there exists a positive constant C independent of h and u such that*

$$h\|u\|_{\infty,K} + h^{1/2}\|u\|_{\Gamma_K} \leq C\|u\|_K.$$

Lemma 4.2. *Suppose $w \in H^{k+1}(\Omega)$, then for any project P_h, which is either P^+, Π_x^-, Π_y^- or P_k, we have*

$$\|w - P_h w\| + h^{1/2}\|w - P_h w\|_{\Gamma_h} \leq Ch^{k+1}.$$

Moreover, the projection P^+ on the Cartesian meshes has the following superconvergence property [33].

Lemma 4.3. *Suppose $w \in H^{k+2}(\Omega)$, then for any $\boldsymbol{\rho} \in \mathbf{W}_h$ we have*

$$|\mathcal{D}(w - P^+ w, \boldsymbol{\rho})| \leq Ch^{k+1}\|w\|_{k+2}\|\boldsymbol{\rho}\|. \tag{4.1}$$

In this paper, we use e to denote the error between the exact and numerical solutions, i.e. $e_c = c_f - c_h$, $e_p = p - p_h$, $\mathbf{e}_u = \mathbf{u} - \mathbf{u}_h$, $\mathbf{e}_s = \mathbf{s} - \mathbf{s}_h$, $\mathbf{e}_z = \mathbf{z} - \mathbf{z}_h$, $e_\phi = \phi - \phi_h$. As the general treatment of the finite element methods, we split the errors into two terms as

$$\begin{array}{lll}
e_c = \xi_c - \eta_c, & \eta_c = P^+ c_f - c_f, & \xi_c = P^+ c_f - c_h, \\
e_p = \xi_p - \eta_p, & \eta_p = P^+ p - p, & \xi_p = P^+ p - p_h, \\
\mathbf{e}_u = \boldsymbol{\xi}_u - \boldsymbol{\eta}_u, & \boldsymbol{\eta}_u = \boldsymbol{\Pi}^- \mathbf{u} - \mathbf{u}, & \boldsymbol{\xi}_u = \boldsymbol{\Pi}^- \mathbf{u} - \mathbf{u}_h, \\
\mathbf{e}_s = \boldsymbol{\xi}_s - \boldsymbol{\eta}_s, & \boldsymbol{\eta}_s = \mathbf{P}_k \mathbf{s} - \mathbf{s}, & \boldsymbol{\xi}_s = \mathbf{P}_k \mathbf{s} - \mathbf{s}_h, \\
\mathbf{e}_z = \boldsymbol{\xi}_z - \boldsymbol{\eta}_z, & \boldsymbol{\eta}_z = \boldsymbol{\Pi}^- \mathbf{z} - \mathbf{z}, & \boldsymbol{\xi}_z = \boldsymbol{\Pi}^- \mathbf{z} - \mathbf{z}_h, \\
e_\phi = \xi_\phi - \eta_\phi, & \eta_\phi = P_k \phi - \phi, & \xi_\phi = P_k \phi - \phi_h.
\end{array}$$

Based on the above notations, it is easy to verify that

$$\mathcal{L}^d(\boldsymbol{\eta}_u, v) = \mathcal{L}^d(\boldsymbol{\eta}_z, v) = 0, \quad \forall v \in Q^k(K). \tag{4.2}$$

Following [24–26,34] with some minor changes, we have the following lemma

Lemma 4.4. *Suppose ξ_c and $\boldsymbol{\xi}_s$ are defined above, we have*

$$\|\nabla \xi_c\| \leq C(\|\boldsymbol{\xi}_s\| + h^{k+1}), \qquad h^{-\frac{1}{2}}\|[\xi_c]\|_{\Gamma_h} \leq C(\|\boldsymbol{\xi}_s\| + h^{k+1}).$$

Let us finish this section by proving the following lemma whose proof was given in [30].

Lemma 4.5. *Let $u \in C^{k+1}(\Omega)$ and $\Pi u \in W_h^k$. Suppose $\|u - \Pi u\| \leq Ch^\kappa$ for some positive constant C and $\kappa \leq k+1$. Then*

$$h\|u - \Pi u\|_\infty + h^{1/2}\|u - \Pi u\|_{\Gamma_h} \leq Ch^\kappa,$$

where the positive constant C does not depend on h.

4.2. A priori error estimate

In this subsection, we would like to make an a priori error estimate assumption that

$$\|c_f - c_h\| + \|\phi - \phi_h\| \leq h, \tag{4.3}$$

which further implies

$$\|c_h\|_\infty + \|\phi_h\|_\infty \leq C \tag{4.4}$$

by hypothesis 4 and Lemma 4.5. Moreover, by Hypothesis 1, we can obtain

$$\|\phi_h\|_\infty \geq C, \quad \kappa^{-1}(\phi_h) \geq C. \tag{4.5}$$

Finally, by Lemma 2.1, we have

$$a_v(\phi_h) \leq C, \quad \kappa^{-1}(\phi_h) \leq C. \tag{4.6}$$

Remark 4.1. The a priori estimate assumption (4.3) holds for small enough h and this choice is heavily based on how large the constant C is in (3.20). Notice that the constant C is independent of h, as long as h is sufficiently small, say $h < H$. Then we can guarantee (4.3) holds for $0 \le t \le T$. Moreover, we will show that, if $h < H$, then the equality of (4.3) cannot happen if $t < T$. However, we still need this estimate to obtain the boundedness of the numerical approximations. This assumption, which will be verified in Section 4.8, is used for the estimate of the convection terms.

4.3. Error equations

In this subsection, we proceed to construct the error equations. From (3.11)–(3.16), we have the following error equations

$$\left(\gamma\frac{\partial e_p}{\partial t}+\frac{\partial e_\phi}{\partial t},\zeta\right)=\mathcal{L}^d(\mathbf{e}_u,\zeta), \tag{4.7}$$

$$\left(\frac{\mu}{\kappa(\phi)}\mathbf{u}-\frac{\mu}{\kappa(\phi_h)}\mathbf{u}_h,\boldsymbol{\theta}\right)=\mathcal{D}(e_p,\boldsymbol{\theta}), \tag{4.8}$$

$$\begin{aligned}((\phi c_f)_t-(\phi_h c_h)_t,v)=&\mathcal{L}^c(\mathbf{u},c_f,v)-\mathcal{L}^c(\mathbf{u}_h,c_h,v)+\mathcal{L}^d(\mathbf{s}_z,v)\\&-\left(A(a_v(\phi)c_f-a_v(\phi_h)c_h),v\right)+(f_p e_c,v),\end{aligned} \tag{4.9}$$

$$(\mathbf{e}_s,\mathbf{w})=\mathcal{D}(e_c,\mathbf{w}), \tag{4.10}$$

$$(\mathbf{e}_z,\boldsymbol{\psi})=(\mathbf{D}(\phi\mathbf{s}-\phi_h\mathbf{s}_h),\boldsymbol{\psi}), \tag{4.11}$$

$$(e_{\phi_t},\beta)=(B(a_v(\phi)c_f-a_v(\phi_h)c_h),\beta), \tag{4.12}$$

for any $v,\ \zeta,\ \beta\in W_h^k$ and $\mathbf{w},\ \boldsymbol{\psi},\ \boldsymbol{\theta}\in\mathbf{W}_h^k$.

4.4. The first energy inequality

In this subsection, we will derive the first energy inequality. Taking $v=\xi_c,\ \mathbf{w}=\boldsymbol{\xi}_z,\ \boldsymbol{\psi}=-\boldsymbol{\xi}_s$ in (4.9), (4.10) and (4.11), respectively, and using Lemma 3.2 and (4.2), we can obtain

$$\left(\phi_h\frac{\partial\xi_c}{\partial t},\xi_c\right)+\left(\mathbf{D}\phi_h\boldsymbol{\xi}_s,\boldsymbol{\xi}_s\right)=R_1+R_2+R_3+R_4+R_5+R_6, \tag{4.13}$$

where

$$\begin{aligned}R_1=&\left(\phi_h\frac{\partial\eta_c}{\partial t},\xi_c\right)-(c_{f_t}\xi_\phi,\xi_c)+(c_{f_t}\eta_\phi,\xi_c)-(\phi_t\xi_c,\xi_c)+(\phi_t\eta_c,\xi_c)\\&-(c_h\xi_{\phi_t},\xi_c)+(c_h\eta_{\phi_t},\xi_c)\\R_2=&(\mathbf{D}\phi_h\boldsymbol{\eta}_s,\boldsymbol{\xi}_s)-(\mathbf{D}\mathbf{s}\xi_\phi,\boldsymbol{\xi}_s)+(\mathbf{D}\mathbf{s}\eta_\phi,\boldsymbol{\xi}_s),\\R_3=&(\mathbf{u}c_f-\mathbf{u}_h c_h,\nabla\xi_c)+\sum_{e\in\Gamma_e}\langle\mathbf{u}c_f-\widehat{\mathbf{u}_h c_h}\cdot\boldsymbol{\nu}_e,[\xi_c]\rangle_e\\R_4=&-\mathcal{D}(\eta_c,\boldsymbol{\xi}_z),\\R_5=&(\boldsymbol{\eta}_s,\boldsymbol{\xi}_z)-(\boldsymbol{\eta}_z,\boldsymbol{\xi}_s)+(f_p e_c,\xi_c),\\R_6=&-(A(a_v(\phi)c_f-a_v(\phi_h)c_h),\xi_c),\end{aligned}$$

where $\Gamma_e=\Gamma_0\cup\partial\Omega_-$ and $\langle u,v\rangle_e=\int_e uv\,ds$. Now, we estimate $R_i\ (i=1,\dots,6)$ term by term. Using hypotheses 4 and (4.4), we can get

$$\begin{aligned}R_1\le&C\|\xi_c\|\left(\|\eta_{c_t}\|+\|\xi_\phi\|+\|\eta_\phi\|+\|\xi_c\|+\|\eta_c\|+\|\xi_{\phi_t}\|+\|\eta_{\phi_t}\|\right)\\\le&C\left(\|\xi_c\|^2+\|\xi_\phi\|^2+\|\xi_{\phi_t}\|^2+h^{2k+2}\right),\end{aligned} \tag{4.14}$$

where the second step requires Lemma 4.2. Use hypotheses 2, 4 and Lemma 4.2 again to obtain

$$\begin{aligned}R_2\le&C\|\boldsymbol{\xi}_s\|\left(\|\boldsymbol{\eta}_s\|+\|\xi_\phi\|+\|\eta_\phi\|\right)\\\le&C\left(\|\xi_\phi\|^2+h^{2k+2}\right)+\epsilon\|\boldsymbol{\xi}_s\|^2.\end{aligned} \tag{4.15}$$

We estimate R_3 by dividing it into three parts

$$R_3=R_{31}+R_{32}-R_{33}, \tag{4.16}$$

where

$$\begin{aligned}R_{31}=&(\mathbf{u}c_f-\mathbf{u}c_h,\nabla\xi_c)+(\mathbf{u}c_h-\mathbf{u}_h c_h,\nabla\xi_c),\\R_{32}=&\frac{1}{2}\sum_{e\in\Gamma_e}\langle(2\mathbf{u}c_f-\mathbf{u}_h^+c_h^+-\mathbf{u}_h^-c_h^-)\cdot\boldsymbol{\nu}_e,[\xi_c]\rangle_e,\end{aligned}$$

$$R_{33} = \frac{1}{2}\sum_{e\in\Gamma_e}\langle\alpha[\xi_c - \eta_c], [\xi_c]\rangle_e.$$

Using hypothesis 4 and (4.4), we have

$$\begin{aligned} R_{31} &\le C\left(\|c_f - c_h\| + \|\mathbf{u} - \mathbf{u}_h\|\right)\|\nabla\xi_c\| \\ &\le C\left(h^{k+1} + \|\boldsymbol{\xi}_u\| + \|\xi_c\|\right)\left(\|\boldsymbol{\xi}_s\| + h^{k+1}\right), \end{aligned} \tag{4.17}$$

where in the first step, we use Schwarz inequality while the second step follows from Lemmas 4.2 and 4.4. C depends on $\|u\|_\infty$ and $\|c_h\|_\infty$. The estimate of R_{32} also requires hypothesis 4 and (4.4),

$$\begin{aligned} R_{32} &= \frac{1}{2}\sum_{e\in\Gamma_e}\langle\left(\mathbf{u}(c_f - c_h^+) + (\mathbf{u} - \mathbf{u}_h^+)c_h^+ + \mathbf{u}(c_f - c_h^-) + (\mathbf{u} - \mathbf{u}_h^-)c_h^-\right)\cdot\boldsymbol{\nu}_e, [\xi_c]\rangle_e \\ &\le C\left(\|c_f - c_h\|_{\Gamma_h} + \|\mathbf{u} - \mathbf{u}_h\|_{\Gamma_h}\right)\|[\xi_c]\|_{\Gamma_h} \\ &\le Ch^{\frac{1}{2}}(\|\eta_c\|_{\Gamma_h} + \|\xi_c\|_{\Gamma_h} + \|\boldsymbol{\eta}_u\|_{\Gamma_h} + \|\boldsymbol{\xi}_u\|_{\Gamma_h})(\|\boldsymbol{\xi}_s\| + h^{k+1}) \\ &\le C\left(h^{k+1} + \|\boldsymbol{\xi}_u\| + \|\xi_c\|\right)\left(\|\boldsymbol{\xi}_s\| + h^{k+1}\right), \end{aligned} \tag{4.18}$$

where in the second step we use Schwarz inequality, the third step follows from Lemma 4.4, the last one requires Lemmas 4.1 and 4.2. Now we proceed to the estimate of R_{33},

$$\begin{aligned} R_{33} &\le C(\|\eta_c\|_{\Gamma_h} + \|\xi_c\|_{\Gamma_h})\|[\xi_c]\|_{\Gamma_h} \\ &\le Ch^{\frac{1}{2}}(\|\eta_c\|_{\Gamma_h} + \|\xi_c\|_{\Gamma_h})(\|\boldsymbol{\xi}_s\| + h^{k+1}) \\ &\le C\left(h^{k+1} + \|\xi_c\|\right)\left(\|\boldsymbol{\xi}_s\| + h^{k+1}\right), \end{aligned} \tag{4.19}$$

where the first step follows from Schwarz inequality, the second step is based on Lemma 4.4, the third one requires Lemma 4.2. Plug (4.17), (4.18) and (4.19) into (4.16) to obtain

$$\begin{aligned} R_3 &\le C\left(h^{k+1} + \|\boldsymbol{\xi}_u\| + \|\xi_c\|\right)\left(\|\boldsymbol{\xi}_s\| + h^{k+1}\right) \\ &\le C\left(\|\boldsymbol{\xi}_u\|^2 + \|\xi_c\|^2 + h^{2k+2}\right) + \epsilon\|\boldsymbol{\xi}_s\|^2. \end{aligned} \tag{4.20}$$

The estimate of R_4 follows from Lemmas 4.3 and 4.2

$$R_4 \le Ch^{k+1}\|c_f\|_{k+2}\|\boldsymbol{\xi}_z\| \le Ch^{2k+2} + \epsilon\|\boldsymbol{\xi}_z\|^2. \tag{4.21}$$

Use Hypotheses 4 and Lemma 4.2 to obtain

$$\begin{aligned} R_5 &\le \|\boldsymbol{\eta}_s\|\|\boldsymbol{\xi}_z\| + \|\boldsymbol{\eta}_z\|\|\boldsymbol{\xi}_s\| + C\|e_c\|\|\xi_c\| \\ &\le C\left(\|\xi_c\|^2 + h^{2k+2}\right) + \epsilon\left(\|\boldsymbol{\xi}_s\|^2 + \|\boldsymbol{\xi}_z\|^2\right). \end{aligned} \tag{4.22}$$

Finally, we estimate R_6,

$$\begin{aligned} R_6 &= (Aa_v(\phi)(c_f - c_h), \xi_c) + (Ac_h(a_v(\phi) - a_v(\phi_h), \xi_c)) \\ &\le C\|\xi_c\|\|c_f - c_h\| + C\|\xi_c\|\|\phi - \phi_h\| \\ &\le C\left(\|\xi_c\|^2 + \|\xi_\phi\|^2 + h^{2k+2}\right), \end{aligned} \tag{4.23}$$

where the second step follows from hypothesis 4, Lemma 2.1 and (4.4), and the last step requires Lemma 4.2. Substituting the estimation (4.14), (4.15), (4.20)–(4.23) into (4.13) and use hypothesis 2 and (4.5), we obtain

$$\begin{aligned} \frac{d\|\xi_c\|^2}{\partial t} + \|\boldsymbol{\xi}_s\|^2 \le{}& C\left(\|\xi_c\|^2 + \|\xi_\phi\|^2 + \|\xi_{\phi_t}\|^2 + \|\boldsymbol{\xi}_u\|^2 + h^{2k+2}\right) \\ &+ \epsilon\left(\|\boldsymbol{\xi}_s\|^2 + \|\boldsymbol{\xi}_z\|^2\right) \end{aligned} \tag{4.24}$$

Now we proceed to eliminate $\|\xi_z\|$ on the right-hand side of the above equation. Take $\boldsymbol{\psi} = \boldsymbol{\xi}_z$ in (4.11) to obtain

$$\begin{aligned} (\boldsymbol{\xi}_z, \boldsymbol{\xi}_z) &= (\boldsymbol{\eta}_z, \boldsymbol{\xi}_z) + (\mathbf{D}(\mathbf{s}\phi - \mathbf{s}_h\phi_h), \boldsymbol{\xi}_z), \\ &= (\boldsymbol{\eta}_z, \boldsymbol{\xi}_z) + (\mathbf{D}\mathbf{s}(\phi - \phi_h), \boldsymbol{\xi}_z) + (\mathbf{D}\phi_h(\mathbf{s} - \mathbf{s}_h), \boldsymbol{\xi}_z), \end{aligned}$$

which further implies

$$\begin{aligned} \|\boldsymbol{\xi}_z\|^2 &\le \|\boldsymbol{\eta}_z\|\|\boldsymbol{\xi}_z\| + C\|\phi - \phi_h\|\|\boldsymbol{\xi}_z\| + C\|\mathbf{s} - \mathbf{s}_h\|\|\boldsymbol{\xi}_z\| \\ &\le C\left(\|\xi_\phi\|^2 + \|\boldsymbol{\xi}_s\|^2 + h^{2k+2}\right) + \epsilon\|\boldsymbol{\xi}_z\|^2, \end{aligned}$$

where in the first step we applied hypotheses 3, 4 and (4.4), the second step follows from Lemma 4.2. Take ϵ to be small, we have

$$\|\boldsymbol{\xi}_z\|^2 \le C\left(\|\xi_\phi\|^2 + \|\boldsymbol{\xi}_s\|^2 + h^{2k+2}\right).$$

Substituting the above equation into (4.24), then integrating with respect to t, we have the first energy inequality

$$\|\xi_c\|^2 + \int_0^t \|\boldsymbol{\xi}_s\|^2\, dt \le C \int_0^t \left(\|\xi_c\|^2 + \|\xi_\phi\|^2 + \|\xi_{\phi_t}\|^2 + \|\boldsymbol{\xi}_u\|^2\right) dt + Ch^{2k+2}. \tag{4.25}$$

4.5. The second energy inequality

In this subsection, we will construct the second energy inequality. Take $\zeta = \xi_p, \boldsymbol{\theta} = \boldsymbol{\xi}_u$ in (4.7) and (4.8), respectively and use Lemma 3.2 and (4.2) to obtain

$$(\gamma \xi_{p_t}, \xi_p) + \left(\frac{\mu}{\kappa(\phi_h)}\boldsymbol{\xi}_u, \boldsymbol{\xi}_u\right) = T_1 + T_2 + T_3, \tag{4.26}$$

where

$$\begin{aligned}
T_1 &= (\gamma \eta_{p_t}, \xi_p) - (\xi_{\phi_t}, \xi_p) + (\eta_{\phi_t}, \xi_p),\\
T_2 &= \left(\frac{\mu}{\kappa(\phi_h)}\boldsymbol{\eta}_u, \boldsymbol{\xi}_u\right) - \left(\mathbf{u}\left(\frac{\mu}{\kappa(\phi)} - \frac{\mu}{\kappa(\phi_h)}\right), \boldsymbol{\xi}_u\right),\\
T_3 &= -\mathcal{D}(\eta_p, \boldsymbol{\xi}_u).
\end{aligned}$$

Now we estimate T_i $(i = 1, 2, 3)$ term by term. Using Lemma 4.2 we have

$$\begin{aligned}
T_1 &\le C\|\xi_p\|\left(\|\eta_{p_t}\| + \|\xi_{\phi_t}\| + \|\eta_{\phi_t}\|\right)\\
&\le C\left(\|\xi_p\|^2 + \|\xi_{\phi_t}\|^2 + h^{2k+2}\right).
\end{aligned} \tag{4.27}$$

The estimate of T_2 requires Lemma 2.1, (4.6) and hypothesis 4,

$$\begin{aligned}
T_2 &\le C\|\boldsymbol{\xi}_u\|\|\boldsymbol{\eta}_u\| + C\|\boldsymbol{\xi}_u\|\|\phi - \phi_h\|\\
&\le C\left(\|\xi_\phi\|^2 + h^{2k+2}\right) + \epsilon\|\boldsymbol{\xi}_u\|^2.
\end{aligned} \tag{4.28}$$

For T_3, we use Lemma 4.3 to obtain

$$T_3 \le Ch^{k+1}\|p\|_{k+2}\|\boldsymbol{\xi}_u\| \le Ch^{2k+2} + \epsilon\|\boldsymbol{\xi}_u\|^2. \tag{4.29}$$

Substituting (4.27)–(4.29) into (4.26), we have

$$\left\|\frac{\mu^{1/2}}{\kappa^{\frac{1}{2}}(\phi_h)}\boldsymbol{\xi}_u\right\|^2 + \frac{1}{2}\frac{d}{dt}\|\gamma^{1/2}\xi_p\|^2 \le C\left(\|\xi_p\|^2 + \|\xi_{\phi_t}\|^2 + \|\xi_\phi\|^2 + h^{2k+2}\right) + \epsilon\|\boldsymbol{\xi}_u\|^2.$$

Integrating the above equation with respect to t and using hypothesis 1, we obtain

$$\|\xi_p\|^2 + \int_0^t \|\boldsymbol{\xi}_u\|^2\, dt \le C\int_0^t \left(\|\xi_p\|^2 + \|\xi_{\phi_t}\|^2 + \|\xi_\phi\|^2\right) dt + Ch^{2k+2}. \tag{4.30}$$

4.6. The third energy inequality

In this subsection, we will derive the third energy inequality. We take $\beta = \xi_\phi$ in (4.12) to obtain

$$\begin{aligned}
(\xi_{\phi_t}, \xi_\phi) &= (\eta_{\phi_t}, \xi_\phi) + \left(Ba_v(\phi)c_f - Ba_v(\phi_h)c_h, \xi_\phi\right)\\
&= (\eta_{\phi_t}, \xi_\phi) + \left(Ba_v(\phi)(c_f - c_h), \xi_\phi\right) + \left(Bc_h(a_v(\phi) - a_v(\phi_h)), \xi_\phi\right),
\end{aligned}$$

which further yields

$$\begin{aligned}
\frac{1}{2}\frac{d}{dt}\|\xi_\phi\|^2 &\le \|\eta_{\phi_t}\|\|\xi_\phi\| + C\|c_f - c_h\|\|\xi_\phi\| + C\|\phi - \phi_h\|\|\xi_\phi\|\\
&\le C\left(\|\xi_\phi\|^2 + \|\xi_c\|^2 + h^{2k+2}\right),
\end{aligned}$$

where we have used Lemma 2.1 and (4.4). Integrating the above inequality with respect to t, we obtain the third energy inequality

$$\|\xi_\phi\|^2 \le C\int_0^t \left(\|\xi_\phi\|^2 + \|\xi_c\|^2\right) dt + Ch^{2k+2}. \tag{4.31}$$

4.7. The fourth energy inequality

In this subsection, we will demonstrate the last energy inequality. We take $\beta = \xi_{\phi_t}$ in (4.12) to obtain

$$\begin{aligned}(\xi_{\phi_t}, \xi_{\phi_t}) &= (\eta_{\phi_t}, \xi_{\phi_t}) + \left(Ba_v(\phi)c_f - Ba_v(\phi_h)c_h, \xi_{\phi_t}\right)\\ &= (\eta_{\phi_t}, \xi_{\phi_t}) + \left(Ba_v(\phi)(c_f - c_h), \xi_{\phi_t}\right) + \left(Bc_h(a_v(\phi) - a_v(\phi_h)), \xi_{\phi_t}\right).\end{aligned}$$

Then we have

$$\begin{aligned}\|\xi_{\phi_t}\|^2 &\le \|\eta_{\phi_t}\|\|\xi_{\phi_t}\| + C\|c_f - c_h\|\|\xi_{\phi_t}\| + C\|\phi - \phi_h\|\|\xi_{\phi_t}\|\\ &\le C\left(\|\xi_c\|^2 + \|\xi_\phi\|^2 + h^{2k+2}\right) + \epsilon\|\xi_{\phi_t}\|^2,\end{aligned}$$

which further yields the last energy inequality

$$\|\xi_{\phi_t}\|^2 \le C\left(\|\xi_c\|^2 + \|\xi_\phi\|^2 + h^{2k+2}\right). \tag{4.32}$$

4.8. Proof of Theorem 3.1

Now we are ready to combine the four energy inequalities and finish the proof of Theorem 3.1.
Firstly, from (4.25) and (4.30), it is easy to derive the following estimate

$$\|\xi_c\|^2 + \|\xi_p\|^2 + \int_0^t \|\boldsymbol{\xi}_s\|^2\, dt \le C\int_0^t \left(\|\xi_c\|^2 + \|\xi_p\|^2 + \|\xi_\phi\|^2 + \|\xi_{\phi_t}\|^2\right) dt + Ch^{2k+2}.$$

Thanks to (4.32), we can eliminate ξ_{ϕ_t} in the above inequality to obtain

$$\|\xi_c\|^2 + \|\xi_p\|^2 + \int_0^t \|\boldsymbol{\xi}_s\|^2\, dt \le C\int_0^t \left(\|\xi_c\|^2 + \|\xi_p\|^2 + \|\xi_\phi\|^2\right) dt + Ch^{2k+2}.$$

Then adding (4.31) and the above inequality, we have

$$\|\xi_c\|^2 + \|\xi_p\|^2 + \|\xi_\phi\|^2 + \int_0^t \|\boldsymbol{\xi}_s\|^2\, dt \le C\int_0^t \left(\|\xi_c\|^2 + \|\xi_p\|^2 + \|\xi_\phi\|^2\right) dt + Ch^{2k+2}.$$

Now, we can employ Gronwall's inequality to obtain

$$\|\xi_c\|^2 + \|\xi_p\|^2 + \|\xi_\phi\|^2 + \int_0^t \|\boldsymbol{\xi}_s\|^2\, dt \le Ch^{2k+2}.$$

Finally, by using the standard approximation result, we obtain (3.20). To complete the proof, let us verify the a priori assumption (4.3). For $k \ge 1$, we can consider h small enough so that $Ch^{k+1} < \frac{1}{2}h$, where C is the constant determined by the final time T. Then define $t^* = \inf\{t : \|c_f - c_h\| + \|\phi - \phi_h\| \ge h\}$, we should have $\|c_f - c_h\| + \|\phi - \phi_h\| = h$ by continuity in time at $t = t^*$. However, if $t^* < T$, Theorem 3.1 implies that $\|c - c_h\| + \|\phi - \phi_h\| \le Ch^{k+1}$ for $t \le t^*$, in particular $h = \|(c - c_h)(t^*)\| + \|(\phi - \phi_h)(t^*)\| \le Ch^{k+1} < \frac{1}{2}h$, which is a contradiction. Therefore, there always holds $t^* \ge T$, and thus the a priori assumption (4.3) is justified.

5. Numerical example

In this section we provide numerical examples to illustrate the accuracy and capability of the method. Time discretization is given as the third order explicit strong-stability-preserving Runge–Kutta method [35].

$$\begin{aligned}\mathbf{w}^{(1)} &= \mathbf{w}^n + \Delta t\mathbf{L}(\mathbf{w}^n),\\ \mathbf{w}^{(2)} &= \frac{3}{4}\mathbf{w}^n + \frac{1}{4}\left(\mathbf{w}^{(1)} + \Delta t\mathbf{L}(\mathbf{w}^{(1)})\right),\\ \mathbf{w}^{n+1} &= \frac{1}{3}\mathbf{w}^n + \frac{2}{3}\left(\mathbf{w}^{(2)} + \Delta t\mathbf{L}(\mathbf{w}^{(2)})\right),\end{aligned}$$

We take the time step to be sufficiently small such that the error in time is negligible compared to spatial error.

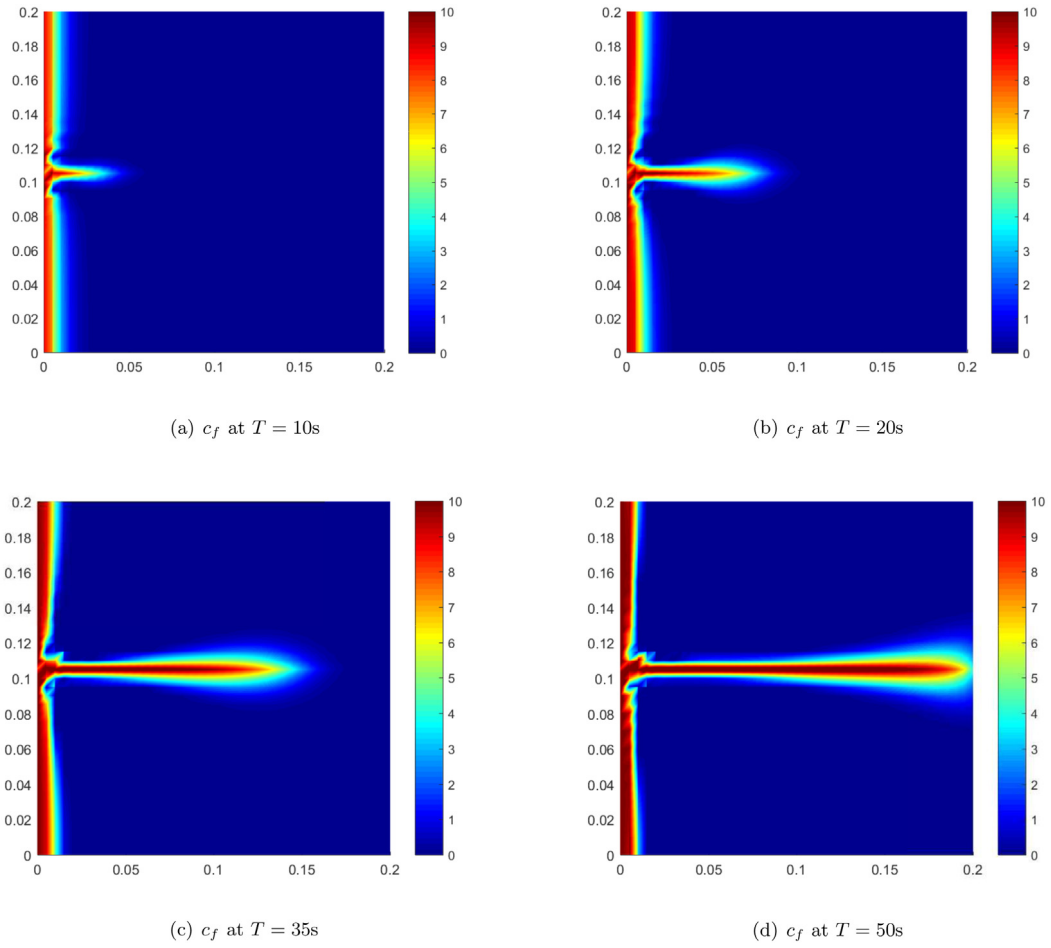

(a) c_f at $T = 10$s (b) c_f at $T = 20$s

(c) c_f at $T = 35$s (d) c_f at $T = 50$s

Fig. 1. Concentration of acid with time evolution.

Example 5.1. We solve (2.1)–(2.4) and the parameters are taken as

$$\mathbf{D} = 10^{-2}\mathbf{I}, K_0 = 1, T = 0.1, \tag{5.33}$$

$$\alpha = k_c = k_s = \mu = f_l = 1, \tag{5.34}$$

$$a_0 = 0.5, \rho_s = 10, \gamma = 0.1, \tag{5.35}$$

where $\mathbf{I}$ is an identity matrix.

The exact smooth solutions are given as

$$p(\mathbf{x}, t) = e^t \sin(2\pi x)\sin(2\pi y), \tag{5.36}$$

$$\phi(\mathbf{x}, t) = t \sin(2\pi x)\cos(2\pi y) + 0.2, \tag{5.37}$$

$$c_f(\mathbf{x}, t) = 0.1e^t \cos(2\pi x)\cos(2\pi y) + 0.2. \tag{5.38}$$

We can calculate the initial conditions and the right hand sides accordingly. Piecewise linear and quadratic tensor product polynomials are used in the LDG scheme. We use uniform meshes with $M \times M$ cells over the computational domain $\Omega = [0, 1] \times [0, 1]$, and compute the numerical approximations at $T = 0.1$. Periodic boundary condition is used in this numerical example. The numerical results are given in Table 1. From the table, we can observe optimal convergence rates, which verifies the results in Theorem 3.1.

Example 5.2. We simulate a real wormhole propagation scenario in petroleum engineering and the parameters are taken as

$$\mathbf{D} = 0, \quad K_0 = 10^{-9}\ \mathrm{m}^2, \quad T = 60\ \mathrm{s}, \tag{5.39}$$

Table 1
Accuracy test for Example 5.1.

	$M \times M$	$\|p - p_h\|_{L^2(\Omega)}$	Order	$\|c_f - c_h\|_{L^2(\Omega)}$	order	$\|\phi - \phi_h\|_{L^2(\Omega)}$	Order
P^1	16×16	1.99E−02	–	1.68E−02	–	1.67E−04	–
	32×32	5.00E−03	1.99	3.92E−03	2.10	4.20E−05	2.00
	64×64	1.25E−03	2.00	7.36E−04	2.41	1.05E−05	2.00
	128×128	3.13E−04	2.00	1.18E−04	2.64	2.62E−06	2.00
P^2	16×16	1.40E−03	–	2.43E−03	–	1.17E−05	–
	32×32	1.76E−04	3.00	2.78E−04	3.13	1.48E−06	3.00
	64×64	2.20E−05	3.00	2.61E−05	3.41	1.85E−07	3.00
	128×128	2.75E−06	3.00	2.14E−06	3.61	2.31E−08	3.00

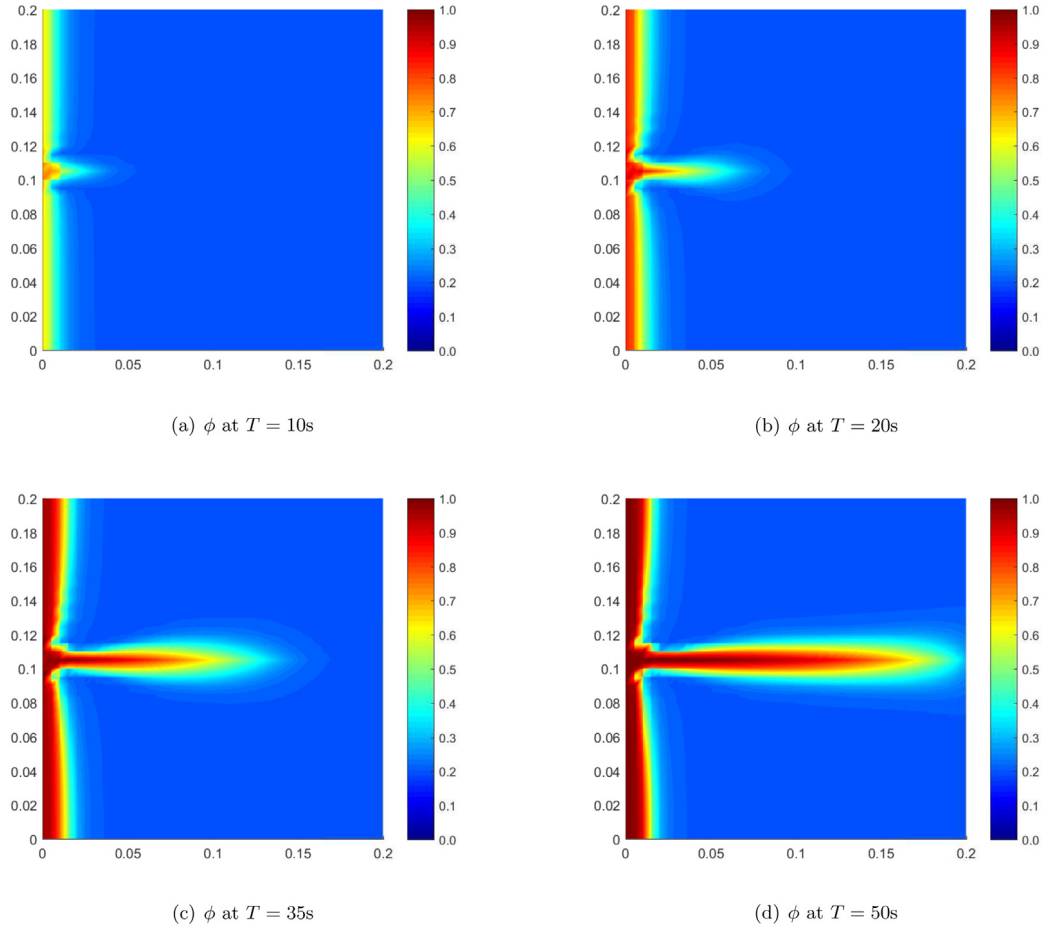

(a) ϕ at $T = 10$s (b) ϕ at $T = 20$s

(c) ϕ at $T = 35$s (d) ϕ at $T = 50$s

Fig. 2. Porosity of rock with time evolution.

$$\alpha = 10\ \text{kg/mol}, \quad k_c = 1\ \text{m/s}, \quad k_s = 10\ \text{m/s}, \tag{5.40}$$

$$\mu = 10^{-2}\ \text{Pa s}, \quad f_l = f_p = 0, \tag{5.41}$$

$$a_0 = 2\ \text{m}^{-1}, \quad \rho_s = 2500\ \text{kg/m}^2, \quad \gamma = 0, \tag{5.42}$$

Computational domain is $\Omega = [0, 0.2\ \text{m}] \times [0, 0.2\ \text{m}]$. Initial concentration of acid and initial porosity of rock in this domain are set to be $c_0 = 0$ and $\phi_0 = 0.2$, respectively. The acid flow is injected to the porous media from the left boundary with a velocity of $u = 0.01$ m/s and drained out of it from the right boundary with the same velocity. Top and bottom boundary conditions are set to be periodic. The concentration of influx acid is 10 mol/m^2. To observe the wormhole propagation, we set a singular area with high porosity and permeability on the middle of the left boundary with size to be 0.01 m $\times$ 0.01 m. The porosity of this singular area is 0.4 and permeability is determined by (2.6) which is about 10^{-8} m^2.

The contour plots of concentration of acid, porosity of rock and pressure with time evolution are shown in the following Figs. 1–3, respectively, from which we can observe the wormhole propagation clearly.

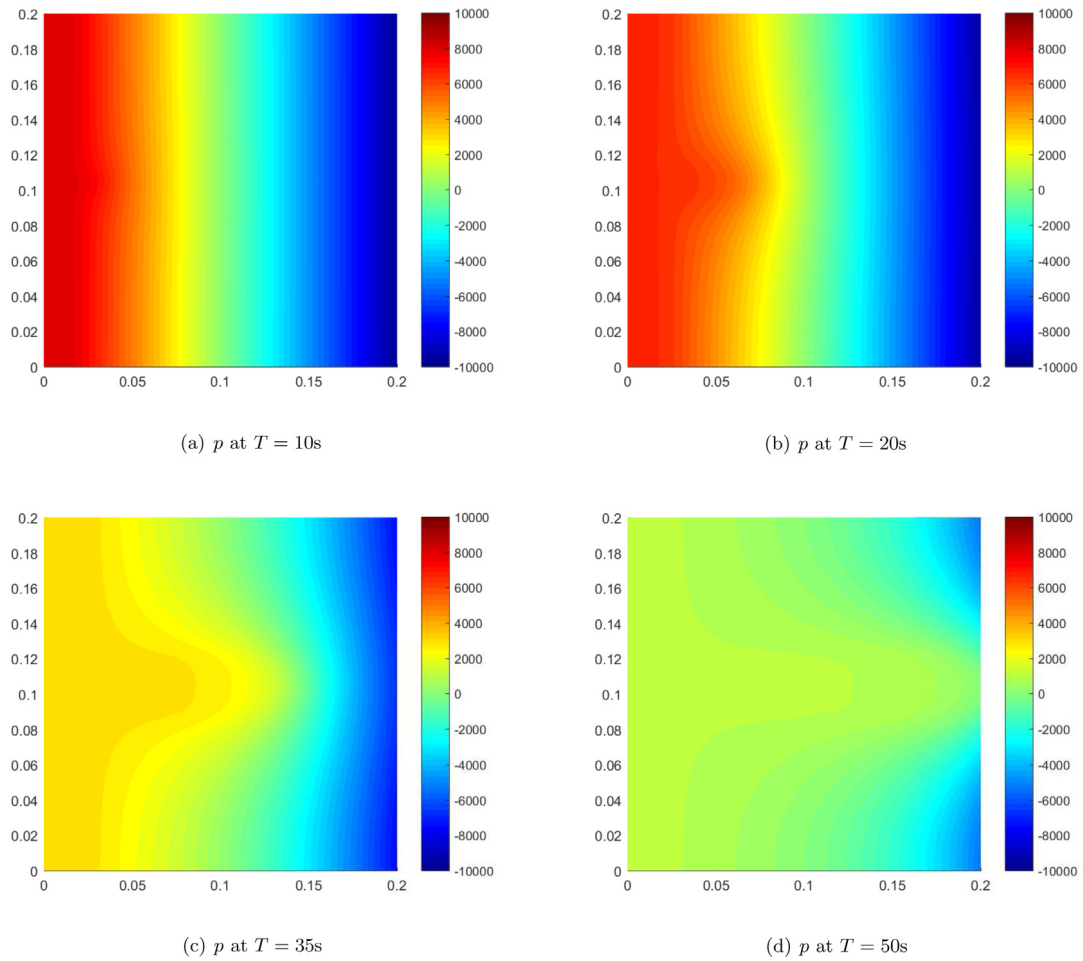

(a) p at $T = 10$s (b) p at $T = 20$s

(c) p at $T = 35$s (d) p at $T = 50$s

Fig. 3. Pressure with time evolution.

6. Concluding remarks

In this paper, we study the compressible wormhole prorogation, and optimal convergence rates are derived. Numerical experiments verify the theoretical analysis.

References

[1] A.S. Smirnov, K.M. Fedorov, A.P. Shevelev, Modeling the acidizing of a carbonate formation, Fluid Dyn. 45 (2010) 779–786.
[2] C.N. Fredd, H.S. Fogler, Influence of transport and reaction on wormhole formation in porous media, Fluid Mech. Transp. Phenom. 44 (1998) 1933–1949.
[3] M.K.R. Panga, M. Ziauddin, Two-scale continuum model for simulation of wormholes in carbonate acidization, AIChE J. 51 (2005) 3231–3248.
[4] P. Szymczak, A.J.C. Ladd, Wormhole formation in dissolving fractures, J. Gophysical Res. 114 (2009) B06203.
[5] M. Liu, S. Zhang, J. Mou, F. Zhou, Wormhole propagation behavior under reservoir condition in carbonate acidizing, Transp. Porous Media 96 (2013) 203–220.
[6] F. Golfier, C. Zarcone, B. Bazin, R. Lenormand, D. Lasseux, M. Quintard, On the ability of a Darcy-scale model to capture wormhole formation during the dissolution of a porous medium, J. Fluid Mech. 457 (2002) 213–254.
[7] C. Zhao, B.E. Hobbs, P. Hornb, A. Ord, S. Peng, L. Liu, Theoretical and numerical analyses of chemical-dissolution front instability in fluid-saturated porous rocks, Int. J. Numer. Anal. Methods Geomech. 32 (2008) 1107–1130.
[8] Y. Wu, A. Salama, S. Sun, Parallel simulation of wormhole propagation with the Darcy-Brinkman-Forchheimer framework, Comput. Geotech. 69 (2015) 564–577.
[9] J. Kou, S. Sun, Y. Wu, Mixed finite element-based fully conservative methods for simulating wormhole propagation, Comput. Methods Appl. Mech. Engrg. 298 (2016) 279–302.
[10] X. Li, H. Rui, Block-centered finite difference method for simulating compressible wormhole propagation, J. Sci. Comput. 74 (2018) 1115–1145.
[11] W.H. Reed, T.R. Hill, Triangular Mesh Method for the Neutron Transport Equation, Technical report LA-UR-73-479, Los Alamos Scientific Laboratory, Los Alamos, NM, 1973.

[12] B. Cockburn, S. Hou, C.W. Shu, The Runge–Kutta local projection discontinuous Galerkin finite element method for conservation laws. IV: The multidimensional case, Math. Comp. 54 (1990) 545–581.
[13] B. Cockburn, S.Y. Lin, C.W. Shu, TVB Runge–Kutta local projection discontinuous Galerkin finite element method for conservation laws. III: One-dimensional systems, J. Comput. Phys. 84 (1989) 90–113.
[14] B. Cockburn, C.W. Shu, TVB Runge–Kutta local projection discontinuous Galerkin finite element method for conservation laws. II: General framework, Math. Comp. 52 (1989) 411–435.
[15] B. Cockburn, C.W. Shu, The Runge–Kutta discontinuous Galerkin method for conservation laws. V: Multidimensional systems, J. Comput. Phys. 141 (1998) 199–224.
[16] B. Cockburn, C.-W. Shu, The local discontinuous Galerkin method for time-dependent convection–diffusion systems, SIAM J. Numer. Anal. 35 (1998) 2440–2463.
[17] F. Bassi, S. Rebay, A high-order accurate discontinuous finite element method for the numerical solution of the compressible Navier–Stokes equations, J. Comput. Phys. 131 (1997) 267–279.
[18] Y. Xu, C.-W. Shu, Local discontinuous Galerkin methods for nonlinear Schrödinger equations, J. Comput. Phys. 205 (2005) 72–97.
[19] Y. Xu, C.-W. Shu, Error estimates of the semi-discrete local discontinuous Galerkin method for nonlinear convection–diffusion and KdV equations, Comput. Methods Appl. Mech. Engrg. 196 (2007) 3805–3822.
[20] J. Yan, C.-W. Shu, Local discontinuous Galerkin methods for partial differential equations with higher order derivatives, J. Sci. Comput. 17 (2002) 27–47.
[21] J. Yan, C.-W. Shu, A local discontinuous Galerkin method for KdV type equations, SIAM J. Numer. Anal. 40 (2002) 769–791.
[22] I.M. Gelfand, Some questions of analysis and differential equations, Am. Math. Soc. Transl. 26 (1963) 201–219.
[23] A.E. Hurd, D.H. Sattinger, Questions of existence and uniqueness for hyperbolic equations with discontinuous coefficients, Trans. Amer. Math. Soc. 132 (1968) 159–174.
[24] H. Wang, C.-W. Shu, Q. Zhang, Stability and error estimates of local discontinuous Galerkin methods with implicit-explicit time-marching for advection-diffusion problems, SIAM J. Numer. Anal. 53 (2015) 206–227.
[25] H. Wang, C.-W. Shu, Q. Zhang, Stability analysis and error estimates of local discontinuous Galerkin methods with implicit-explicit time-marching for nonlinear convection–diffusion problems, Appl. Math. Comput. 272 (2016) 237–258.
[26] H. Wang, S. Wang, Q. Zhang, C.-W. Shu, Local discontinuous Galerkin methods with implicit-explicit time marching for multi-dimensional convectiondiffusion problems, ESAIM Math. Model. Numer. Anal. 50 (2016) 1083–1105.
[27] H. Guo, Q. Zhang, J. Wang, Error analysis of the semi-discrete local discontinuous galerkin method for compressible miscible displacement problem in porous media, Appl. Math. Comput. 259 (2015) 88–105.
[28] H. Guo, F. Yu, Y. Yang, Local discontinuous Galerkin method for incompressible miscible displacement problem in porous media, J. Sci. Comput. 71 (2017) 615–633.
[29] F. Yu, H. Guo, N. Chuenjarern, Y. Yang, Conservative local discontinuous Galerkin method for compressible miscible displacements in porous media, J. Sci. Comput. 73 (2017) 1249–1275.
[30] X. Li, C.-W. Shu, Y. Yang, Local discontinuous Galerkin methods for Keller–Segel chemotaxis model, J. Sci. Comput. 73 (2017) 943–967.
[31] S. Mauran, L. Rigaud, O. Coudevylle, Application of the Carman-Kozeny correlation to a highporosity and anisotropic consolidated medium: The compressed expanded natural graphite, Transp. Porous Media 43 (2001) 355–376.
[32] P. Ciarlet, The Finite Element Method for Elliptic Problem, North Holland, 1975.
[33] P. Castillo, B. Cockburn, I. Perugia, D. Schötzau, Superconvergence of the local discontinuous Galerkin method for elliptic problems on cartesian grids, SIAM J. Numer. Anal. 39 (2001) 264–285.
[34] Y. Yang, C.-W. Shu, Analysis of optimal superconvergence of local discontinuous Galerkin method for one-dimensional linear parabolic equations, J. Comput. Math. 33 (2015) 323–340.
[35] C.-W. Shu, S. Osher, Efficient implementation of essentially non-oscillatory shock-capturing schemes, J. Comput. Phys. 77 (1988) 439–471.